Scripta Materialia 128 (2017) 45–48

Contents lists available at ScienceDirect

Scripta Materialia

journal homepage: www.elsevier.com/locate/scriptamat

Regular Article

Elastic properties of the sigma W-Re phase: A first principles investigation

G. Bonny [a,*], A. Bakaev [a], D. Terentyev [a], Yu.A. Mastrikov [b]

[a] SCK•CEN, Nuclear Materials Science Institute, Boeretang 200, B-2400, Mol, Belgium
[b] University of Latvia, Institute for Solid State Physics, Kengaraga str. 8, Riga, Latvia

ARTICLE INFO

Article history:
Received 13 July 2016
Received in revised form 15 September 2016
Accepted 29 September 2016
Available online 13 October 2016

Keywords:
Sigma phase
Elastic constants
Density functional theory
Sublattice model

ABSTRACT

We perform density functional theory (DFT) calculations to obtain the formation enthalpy and six independent elastic constants for the 32 possible occupations of the five non-equivalent sites of the σ-phase. The obtained results suggest linear correlation between bulk modulus and Re concentration and between shear modulus and formation enthalpy. The results are used to parameterize a sublattice model with ideal mixing on each sublattice for the free energy and elastic constants. The model allows one to predict the equilibrium composition on each sublattice and hence elastic constants as a function of global Re concentration and temperature of the W-Re alloy.

The performance of several classes of materials, such as, W-based alloys, industrial steels and Ni-based super alloys, is often limited by the precipitation of topologically closed packed (tcp) phases. The formation of tcp phases, also known as Frank-Kasper (FK) phases [1], leads to the embrittlement of the material [2–4].

The precipitation of tcp phases and their role in embrittlement are of essential concern for the design of plasma-facing components using W-based alloys. Indeed, tungsten is the material of choice for the diverter in ITER and is considered as the first wall material for the DEMO fusion reactors [5]. Although commercially pure W is considered as baseline material for these applications, fluxes of neutrons generated in the fusion reactions will result in the generation of rhenium (Re), whose amount may enrich W up to several percent after five years of operation under the envisaged exploitation conditions [6,7].

Even though the solubility of Re in W is substantial (~25% below 1000 °C [8]), tcp phases in the form of σ and χ-phases are known to form in alloys containing as little as 5% Re under the influence of neutron irradiation [9]. In addition, post-irradiation experiments clearly point to a strong increase of the hardness associated not only to conventional radiation defects (loops and voids), but also to the formation of Re precipitates [10].

In the literature many works are available with respect to the energetic description of both σ and χ-phases [11–15], but very little is known about their elastic properties. However, the latter play an important role in the governing mechanisms of embrittlement, originating from the suppression of dislocation motion. Consequently, the characterization of the resistance of the Re-induced σ and χ-phases requires the assessment of their specific structure and elastic properties. As the σ-phase is the first one appearing in the W-Re phase diagram at the W-rich side [16], here, we focus on the elastic properties of the σ W-Re phase by means of first principles density functional theory (DFT) calculations.

The σ-phase ($D8_b$) is a tetragonal phase described by the $P4_2/mnm$ space group with five non-equivalent positions, namely, I, II, III, IV and V (Wyckoff positions 2*a*, 4*f*, $8i_1$, $8i_2$ and 8*j*, respectively). The σ-phase (and tcp phases in general) exist in a large homogeneity range without a fixed stoichiometry. However, complete disorder is never observed as the non-equivalent sites exhibit a preferential occupancy.

With this notion both formation enthalpy (H_f) and elastic constants ($C_{11}, C_{12}, C_{13}, C_{33}, C_{44}, C_{66}$) are expressed in a sublattice model with ideal mixture on each of the five sublattices. Within this approximation the elastic constants (similar for H_f) are given as,

$$C_{ij}(x_{\mathrm{Re}}) = \sum_{k,l,m,n,o=\mathrm{W,Re}} y_k^{\mathrm{I}}\, y_l^{\mathrm{II}}\, y_m^{\mathrm{III}}\, y_n^{\mathrm{IV}}\, y_o^{\mathrm{V}}\, C_{ij}(k,l,m,n,o), \tag{1}$$

with x_{Re} the global atomic fraction of Re, $C_{ij}(k,l,m,n,o)$ the elastic constant corresponding to a compound with (k,l,m,n,o) site occupancy and y_p^s the fractional site occupancy of species *p* on sublattice *s* that minimizes the total Gibbs free energy, *G*. When neglecting all phonon and magnetic contributions to the total Gibbs free energy and assuming ideal mixing on each sublattice, *G* is given as,

$$G(x_{\mathrm{Re}},T) = \sum_{k,l,m,n,o=\mathrm{W,Re}} y_k^{\mathrm{I}}\, y_l^{\mathrm{II}}\, y_m^{\mathrm{III}}\, y_n^{\mathrm{IV}}\, y_o^{\mathrm{V}}\, H_f(k,l,m,n,o) + \sum_{k=\mathrm{W,Re}} x_k H_k^{\mathrm{ref}} + \frac{k_B T}{N_{\mathrm{cell}}} \sum_s m_s \sum_{k=\mathrm{W,Re}} y_k^s \ln\left(y_k^s\right), \tag{2}$$

* Corresponding author.
E-mail address: gbonny@sckcen.be (G. Bonny).

http://dx.doi.org/10.1016/j.scriptamat.2016.09.039
1359-6462/

Table 1
Formation enthalpy (H_f) (eV/at.), equilibrium atomic volume (V_0) (Å^3/at.), elastic constants (C_{ij}) (GPa), bulk modulus B_V (GPa) and shear modulus G_V (GPa) for all considered compounds.

I	II	III	IV	V	H_f	V_0	C_{11}	C_{12}	C_{13}	C_{33}	C_{44}	C_{66}	B_V	G_V
W	W	W	W	W	0.176	16.27	466	259	180	545	93	95	301	113
Re	W	W	W	W	0.145	16.22	478	258	180	549	93	93	305	115
W	Re	W	W	W	0.193	16.12	464	270	189	526	86	82	305	104
Re	Re	W	W	W	0.167	16.08	474	272	191	528	87	83	309	106
W	W	W	W	Re	0.165	15.97	481	258	198	563	95	88	315	114
W	W	W	Re	W	0.058	15.93	525	261	203	553	102	107	326	124
W	W	Re	W	W	0.147	15.96	483	267	201	526	79	95	315	106
Re	W	W	W	Re	0.133	15.90	497	252	200	567	95	95	319	118
Re	W	W	Re	W	0.029	15.83	533	246	205	562	105	122	327	131
Re	W	Re	W	W	0.114	15.88	502	261	203	524	84	100	318	111
W	Re	W	W	Re	0.173	15.84	490	262	203	552	87	75	319	108
W	Re	W	Re	W	0.073	15.77	519	258	207	561	101	102	327	123
W	Re	Re	W	W	0.170	15.85	484	261	208	511	77	89	315	102
Re	Re	W	W	Re	0.149	15.77	498	260	213	547	91	87	324	111
Re	Re	W	Re	W	0.048	15.71	535	255	206	573	108	120	331	132
Re	Re	Re	W	W	0.142	15.77	501	263	212	529	85	96	323	110
W	W	W	Re	Re	0.059	15.64	540	239	216	587	105	123	334	133
W	W	Re	W	Re	0.138	15.69	510	240	227	526	75	108	326	108
W	W	Re	Re	W	0.061	15.61	549	245	221	550	93	128	336	127
Re	W	W	Re	Re	0.038	15.55	548	242	222	605	110	127	341	137
Re	W	Re	W	Re	0.110	15.62	578	303	262	525	78	114	370	111
Re	W	Re	Re	W	0.035	15.53	561	244	226	574	97	142	343	134
W	Re	W	Re	Re	0.073	15.51	546	252	227	588	102	111	344	128
W	Re	Re	W	Re	0.162	15.55	518	232	275	510	66	101	346	98
W	Re	Re	Re	W	0.089	15.49	551	241	229	550	85	89	339	115
Re	Re	W	Re	Re	0.056	15.43	549	257	229	600	112	112	348	133
Re	Re	Re	W	Re	0.139	15.41	525	244	265	485	75	107	342	102
Re	Re	Re	Re	W	0.067	15.42	557	256	231	568	92	135	347	128
W	W	Re	Re	Re	0.082	15.39	554	230	264	520	74	128	349	113
Re	W	Re	Re	Re	0.067	15.30	554	241	271	531	75	120	356	111
W	Re	Re	Re	Re	0.110	15.26	546	235	285	491	70	105	355	101
Re	Re	Re	Re	Re	0.096	15.18	550	249	294	515	76	103	365	103

with H_k^{ref} the reference enthalpy of species k in its ground state lattice structure (bcc for W and hcp for Re), k_B Boltzmann's constant, T the absolute temperature, N_{cell} the number atoms in the unit cell (here 30), m_s the multiplicity of site s (2, 4, 8, 8, 8 for I, II, III, IV, V, respectively) and $H_f(k,l,m,n,o)$ the formation enthalpy corresponding to a compound with (k,l,m,n,o) site occupancy. Here the reference enthalpy, H_k^{ref}, is taken independent from temperature following the cohesive energy given in [17] ($H_{\mathrm{W}}^{\mathrm{ref}} = -8.90$ eV and $H_{\mathrm{Re}}^{\mathrm{ref}} = -8.03$ eV). In Eq. (2) the first two terms give the enthalpy and the last term provides the configurational entropy for ideal mixing on each sublattice. In both Eqs. (1) and (2), $C_{ij}(k,l,m,n,o)$ and $H_f(k,l,m,n,o)$ are obtained solely from DFT calculations at 0 K. We emphasize that within this thermodynamic model the effects of temperature are only carried by the configurational entropy.

The DFT calculations to obtain all 32 permutations of $C_{ij}(k,l,m,n,o)$ and $H_f(k,l,m,n,o)$ were performed using the Vienna ab initio simulation package (VASP 5.3) [18,19], which is a plane-wave DFT code with the Projector Augmented Wave (PAW) method implemented [20,21]. We used standard PAW potentials supplied with VASP and the Generalized Gradient Approximation (GGA) with Perdew-Burke-Ernzerhof exchange-correlation functional [22]. The calculations were non-spin-polarized and for W and Re potentials with 6 and 7 valence electrons were applied, respectively.

The Methfessel-Paxton method was used to introduce finite temperature smearing with a width of 0.3 eV, which proved enough for convergence of the total energy. The plane-wave cut-off energy was set to 800 eV for formation enthalpy calculations and 400 eV for the elastic constants. The Monkhorst-Pack scheme was applied for Brillouin zone sampling and k-point meshes of $8 \times 8 \times 15$ k-points and $4 \times 4 \times 11$ k-points were used for the formation enthalpy and elastic constants, respectively. These settings yield results consistent with [13,14] and proved sufficient for an enthalpy convergence of 2 meV/at. and 2% relative error in the elastic constants (compared to a $20 \times 20 \times 20$ k-points mesh and 1500 eV cut-off energy). The total energy was calculated in a periodic unit cell containing 30 atoms describing the σ-phase. In the calculations cell shape, volume and ionic positions were relaxed. Ionic relaxation was performed using the conjugate gradient algorithm with a force convergence criterion of 0.03 eV/Å.

The results of the DFT calculations are summarized in Table 1 and are in good agreement with [13,14]. The formation enthalpy (with DFT reference enthalpy $H_{\mathrm{W}}^{\mathrm{bcc}} = -13.018$eV/at. and $H_{\mathrm{Re}}^{\mathrm{hcp}} = -12.425$ eV/at.), relaxed volume (V_0) and six independent elastic constants are provided for all 32 possible occupancies of the five sublattices by W and Re. We note that even though cell shape relaxation was allowed, all considered compounds kept their tetragonal symmetry after relaxation. As the individual elastic constants are difficult to discuss, we computed the Voigt average for both bulk (B_V) and shear modulus (G_V). The latter values provide a measure for the resistance against uniform deformation and

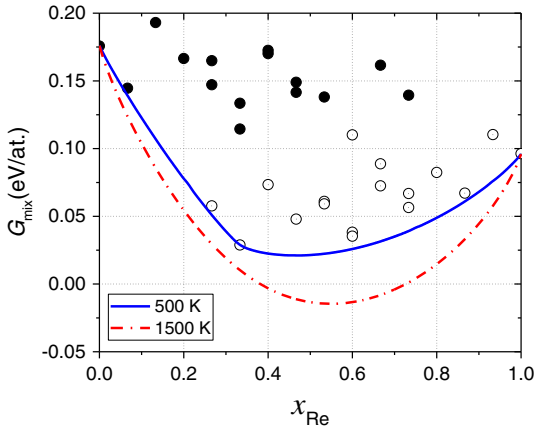

Fig. 1. Free energy of mixing, G_{mix}, as a function of x_{Re} at 500 and 1500 K. The symbols correspond to DFT data at 0 K for the 32 considered compounds. Filled symbols correspond to $H_f > 0.111$ eV/at., while open symbols correspond to $H_f \leq 0.111$ eV/at.

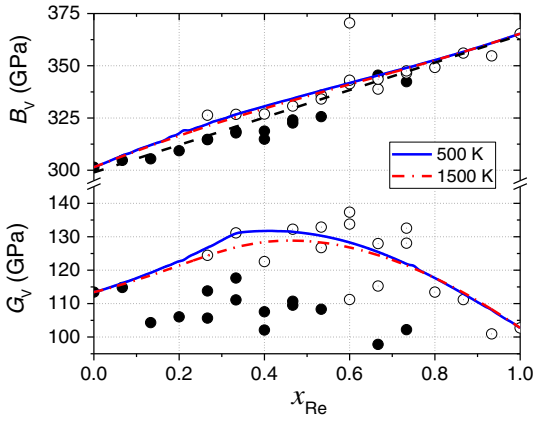

Fig. 2. Voigt average of the bulk B_V and shear modulus G_V based on the sublattice model with ideal mixing at 500 and 1500 K and the 32 compounds considered in the DFT calculations. Filled symbols correspond to H_f>0.111 eV/at., while open symbols correspond to H_f≤0.111 eV/at.

shear deformation of a poly crystal. For a tetragonal crystal, they are given as,

$$B_V = \frac{1}{9}[(2C_{11} + C_{33}) + 2(C_{12} + 2C_{13})], \quad (3)$$

$$G_V = \frac{1}{15}[(2C_{11} + C_{33}) - (C_{12} + 2C_{13}) + 3(2C_{44} + C_{66})]. \quad (4)$$

The formation enthalpy and Voigt average of both bulk and shear modulus presented in Table 1 are summarized in Fig. 1 and Fig. 2, respectively. The data points are separated in two groups: open symbols indicate compounds with low formation enthalpy (H_f≤0.111 eV/at.), while filled symbols indicate compounds with high formation enthalpy (H_f>0.111 eV/at.). The reason for this grouping is explained later. Prior to discussing the results from the thermodynamic model, we attempt to identify some correlations in the DFT data.

From both Figs. 1 and 2 it is clear that there is no correlation between x_{Re} and H_f or G_V. However, with a correlation factor of $R^2 = 0.83$ there is a linear correlation between B_V and x_{Re}. To rationalize this correlation we plotted both x_{Re} and B_V as a function of formation enthalpy density, ρ_f (see Fig. 3a), which is the ratio between H_f and V_0. With a correlation factor of $R^2 = 0.84$ there is a linear correlation between B_V and ρ_f. This is consistent with previous observations where a correlation between bulk modulus and energy density was found for pure elements [23].

Also between ρ_f and x_{Re} the correlation is strong ($R^2 = 0.88$), hence the linear correlation between B_V and x_{Re}.

As shown in Fig. 2, on the other hand, there is no obvious correlation between G_V and x_{Re}. However, when G_V is plotted against H_f (see Fig. 3b), linear correlation ($R^2 = 0.76$) is observed for compounds with H_f≤0.111 eV/at. Whereas B_V describes the material's response under uniform tension or compression, G_V gives the response to shear deformation. Since there is (almost) no volumetric change associated to shear deformation, G_V is solely determined by the bonding strength between the atoms. In turn, H_f is a good measure for the bonding strength, i.e., lower values of H_f indicate stronger bonding. This explains the linear correlation between G_V and H_f when only the most stable compounds are considered (H_f≤0.111 eV/at.). For less stable compounds the correlation is lost.

On the other hand, besides the bonding strength B_V also includes effects of volumetric change, and therefore no simple correlation between B_V and H_f is found, as illustrated in Fig. 3b.

Following the discussion of the DFT results at 0 K, we now focus on the results of the thermodynamic calculations. As an illustration of the accuracy of the sublattice model with ideal mixing on each sublattice, we present the optimized site occupation fractions (y^s_{Re}) for each of the five sublattices s as a function of x_{Re} at 1500 K in Fig. 4. The curves were obtained by minimizing the free energy (see Eq. (2)) with respect to y^s_{Re} at the given temperature. We note that the curves predicted by the model are in excellent agreement with the experimental data points from [11] and are consistent with the models developed by Berne et al. [11,12] and Crivello et al. [13,14]. Clearly sites I and IV have a preference for Re occupancy while sites II, III and V prefer W occupancy. The latter is explained by the fact that Re behaves as undersized compared to W [14]. In turn it is known that undersized atoms prefer to locate in sites with a lower coordination number (12 for sites I and IV) while oversize atoms prefer sites with a higher coordination number (15 for site II and 14 for sites III and V).

The Gibbs free energy of mixing, G_{mix}, at 500 and 1500 K based on the minimization of the Gibbs free energy is superposed in Fig. 1. For the lowest temperature G_{mix} follows the convex hull around the lowest H_f closely. At higher temperature the effect of configurational entropy shifts the minimum ($x_{Re} \approx 0.5$) to higher Re content.

Given the $\{y^s_{Re}\}$ from the free energy minimization, the corresponding B_V and G_V are superposed in Fig. 2. From the figure it is clear that both B_V and G_V do not change significantly with temperature. Thus, the influence of temperature via configurational entropy is negligible. When including phonon contributions, however, both B_V and G_V are expected to reduce significantly.

In Table 2 a comparison between the σ-phase and bcc W and hcp Re is provided for B_V and G_V. While the difference between the σ-phase and

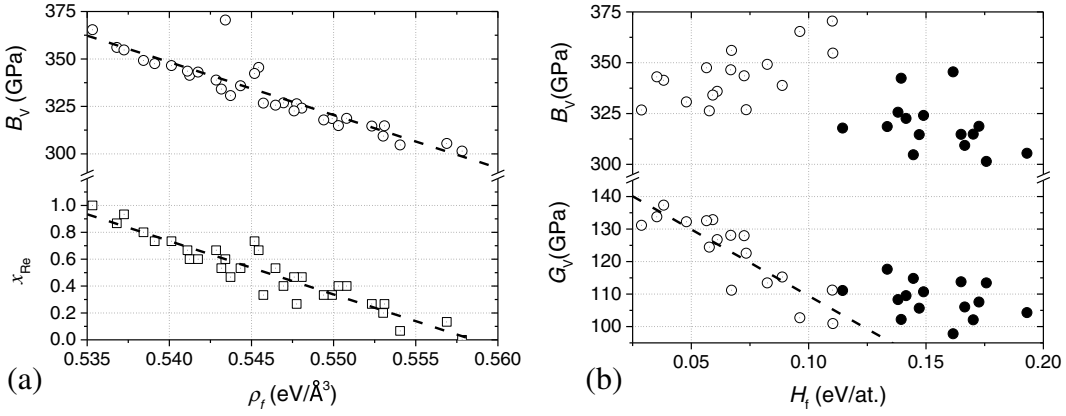

Fig. 3. (a) Voigt average of the bulk modulus B_V and x_{Re} corresponding to the 32 compounds as a function of ρ_f; (b) Voigt average of the bulk B_V and shear modulus G_V for the 32 compounds calculated by DFT as a function H_f. Filled symbols correspond to H_f>0.111 eV/at., while open symbols correspond to H_f≤0.111 eV/at.

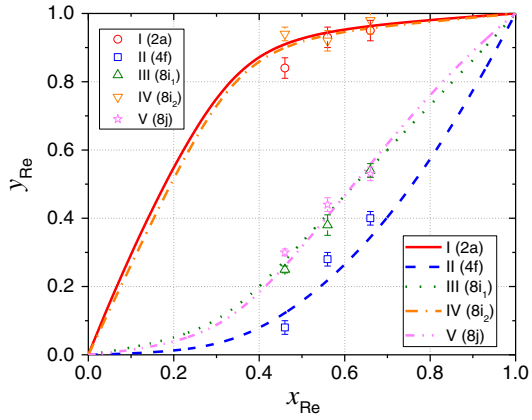

Fig. 4. Fractional site occupation of Re (y^s_{Re}) for the different non-equivalent sites s as a function of x_{Re} at 1500 K. The symbols show experimental data [11].

true ground state structure for B_V is negligible, G_V reduces by 30% and 43% for W and Re, respectively. As G_V is a measure for the resistance against shear deformation, we can conclude that σ W or Re is significantly softer than in their true ground state lattice. Given the limited variation of G_V for bcc W-10%Re ($G_V = 163$ GPa) [24] this conclusion likely holds for a wide composition range in the bcc W-Re phase.

Thus, the experimentally observed hardening and embrittlement due to σ-phase precipitation is unlikely to originate from the matrix-precipitate shear modulus misfit. It is rather linked to the non-coherent structure of the matrix-precipitate interface, which implies impenetrable behavior of the σ-phase precipitate and overall resulting in the strong pinning of the dislocations that must overcome such inclusions by either Orowan or cross-slip mechanisms. Earlier, this phenomenon was studied and proven (both experimentally and theoretically) for Fe-Cu alloys [26].

In conclusion, the DFT results suggest linear correlation between the Voigt average of the bulk modulus and Re concentration and between the Voigt average of the shear modulus and formation enthalpy. At finite temperature we observe that neither bulk nor shear modulus change due to temperature effects associated with the configurational entropy. The bulk modulus changes almost linearly with the composition and the shear modulus reaches a maximum value for around 50% Re, with a value about 20% higher as compared to σ W and σ Re.

Acknowledgements

This work has been carried out within the framework of the EUROfusion Consortium and has received funding from the Euratom research and training programme 2014–2018 under grant agreement No 633053. The views and opinions expressed herein do not necessarily reflect those of the European Commission.

Table 2
Comparison of B_V and G_V between the σ-phase and true ground states of W and Re.

		B_V (GPa)	G_V (GPa)
W	bcc	316 [24]	161 [24]
	σ	301	113
Re	hcp	362 [25]	180 [25]
	σ	365	103

References

[1] F.C. Frank, J.S. Kasper, Acta Crystallogr. 11 (1958) 184.
[2] D. Peckner, M. Burnstein, Handbook of Stainless Steels, McGraw-Hill, New York, 1977.
[3] B.D. Bryskin, J.-C. Carlén, Mater. Manuf. Process. 11 (1996) 67.
[4] C.M. Rae, R.C. Reed, Acta Mater. 49 (2001) 4113.
[5] H. Bolt, V. Barabash, W. Krauss, J. Linke, R. Neu, S. Suzuki, N. Yoshida, J. Nucl. Mater. 329–333 (2004) 66.
[6] G.A. Cottrell, R. Pampin, N.P. Taylor, Fusion Sci. Technol. 50 (2006) 89.
[7] M.R. Gilbert, S.L. Dudarev, S. Zheng, L.W. Packer, J.-C. Sublet, Nucl. Fusion 52 (2012) 083019.
[8] R.I. Jaffee, C.T. Sims, J.J. Harwood, The Effect of Rhenium on the Fabricability and Ductility of Molybdenum and Tungsten, 3rd Plansee Seminar Proceedings, 1958, Pergamon Press, New York, 1959 380–411.
[9] T. Tanno, M. Fukuda, S. Nogami, A. Hasegawa, Mater. Trans. 52 (2011) 1447.
[10] M. Fukuda, T. Tanno, S. Nogami, A. Hasegawa, Mater. Trans. 53 (2012) 2145.
[11] C. Berne, M. Sluiter, Y. Kawazoe, T. Hansen, A. Pasturel, Phys. Rev. B 64 (2001) 144103.
[12] C. Berne, M. Sluiter, Y. Kawazoe, A. Pasturel, J. Phys. Condens. Matter 13 (2001) 9433.
[13] J.-C. Crivello, J.-M. Joubert, J. Phys. Condens. Matter 22 (2010) 035402.
[14] J.-C. Crivello, A. Breidi, J.-M. Joubert, Inorg. Chem. 52 (2013) 3674.
[15] M. Palumbo, S.G. Fries, T. Hammerschmidt, T. Abe, J.-C. Crivello, A. Al Hasan Breidi, J.-M. Joubert, R. Drautz, Comp. Mater. Sci. 81 (2014) 433.
[16] T.B. Massalski, Binary Alloy Phase Diagram, second edition ASM International, 2007.
[17] C. Kittel, Introduction to Solid State Physics, seventh edition John Wiley & Sons, New York, 1996.
[18] G. Kresse, J. Hafner, Phys. Rev. B 47 (1993) RC558.
[19] G. Kresse, J. Furthmuller, Phys. Rev. B 54 (1996) 11169.
[20] P.E. Blöchl, Phys. Rev. B 50 (1994) 17953.
[21] G. Kresse, D. Joubert, Phys. Rev. B 59 (1999) 1758.
[22] J.P. Perdew, K. Burke, M. Ernzerhof, Phys. Rev. Lett. 78 (1997) 1396.
[23] S. Wacke, T. Górecki, C. Górecki, K. Książek, J. Phys. Conf. Ser. 289 (2011) 012020.
[24] R.A. Ayres, G.W. Shannette, D.F. Stein, J. Appl. Phys. 46 (1975) 1526.
[25] M.L. Shepard, J.F. Smith, J. Appl. Phys. 36 (1965) 1447.
[26] B. Minov, D. Terentyev, W. Van Renterghem, Y. Osetsky, M.J. Konstantinovic, Mater. Sci. Eng. A 597 (2014) 46.